Available online at www.sciencedirect.com
ScienceDirect
European Journal of Medicinal Chemistry 43 (2008) 1095–1104
EUROPEAN JOURNAL OF MEDICINAL CHEMISTRY
http://www.elsevier.com/locate/ejmech

Short communication

Synthesis and structure–antibacterial activity of triazolyl oxazolidinones containing long chain acyl moiety

Oludotun A. Phillips [a,*], Edet E. Udo [b], Santhosh M. Samuel [a]

[a] *Department of Pharmaceutical Chemistry, Faculty of Pharmacy, Kuwait University, P.O. Box 24923, Safat 13110, Kuwait*
[b] *Department of Microbiology, Faculty of Medicine, Kuwait University, P.O. Box 24923, Safat 13110, Kuwait*

Received 22 April 2007; received in revised form 9 July 2007; accepted 9 July 2007
Available online 27 July 2007

Abstract

A series of new piperazinyl 5-triazolylmethyl oxazolidinones containing long chain acyl group at the piperazine N-4-position were synthesized and evaluated against a panel of standard and clinical isolates of Gram-positive and Gram-negative bacteria. Derivatives having long chain acyl groups with nine or more number of carbon atoms showed significant decrease in antibacterial activity. Antibacterial activity correlated positively with heat of formation of the compounds, but correlated negatively with Clog *P* values, surface area, ovality and molecular volume. However, no significant correlation was observed between activity and E_{LUMO}, E_{HOMO} and dipole, respectively.

Keywords: Antibacterial activity; Heat of formation; Linezolid; Molecular descriptors; Oxazolidinones; Structure–activity relationships

1. Introduction

Although the judicious use of antibacterial agents is an important approach in attempts to control the emergence of bacterial resistance, the discovery and development of newer agents are desirable for the successful treatment of infections caused by resistant pathogenic bacteria. Among the new agents under development, only the oxazolidinone, cationic peptide and lipopeptide antibiotics can be truly regarded as novel mechanism agents [1]. A clinically useful member of the oxazolidinone class of antibacterial agents, linezolid (Fig. 1) is highly effective against multi-drug resistant Gram-positive bacteria, including methicillin-resistant *Staphylococcus aureus* (MRSA), methicillin-resistant coagulase-negative staphylococci (MR-CNS), penicillin-resistant *Streptococcus pneumoniae* (PRSP) and vancomycin-resistant enterococcus (VRE) [2–4], which have been identified as the most prevalent bacteria species isolated from inpatient specimens in USA [5]. These organisms are also reported to be resistant to at least three classes of antibacterial agents commonly used for therapy. Oxazolidinones, linezolid and eperezolid (Fig. 1) exhibit a unique mechanism of action that involves interference with the binding of mRNA to the ribosomes at the initiation phase of translation. They explicitly inhibit the formation of the initiation complex in bacterial translation system thus preventing formation of the *N*-formylmethionyl-*t*RNA-ribosome-*m*RNA ternary complex ($tRNA^{fMet}$-*m*RNA) [6–8]. Although linezolid has demonstrated clinical success, recent reports on emerging linezolid-resistant *S. aureus* [9] and *Enterococcus* spp. [10–12] in hospital isolates suggest an increasing need for new, more effective and safer antibacterial agents. These situations continue to serve as impetus for the development of novel and more effective antibacterial agents.

Recent developments in the modification of the C-5 position of the oxazolidinones have highlighted the bioisosteric replacement of the acetamide group by a triazole moiety [13–15], which is exemplified by PH-027, and compounds of general structures **1** and **2** (Fig. 1). We have previously

* Corresponding author. Tel.: +965 498 6070; fax: +965 534 2807.
E-mail addresses: dphillips@hsc.edu.kw (O.A. Phillips), edet@hsc.edu.kw (E.E. Udo), santhosh_samuel@hotmail.com (S.M. Samuel).

0223-5234/$ - see front matter © 2007 Elsevier Masson SAS. All rights reserved.
doi:10.1016/j.ejmech.2007.07.006

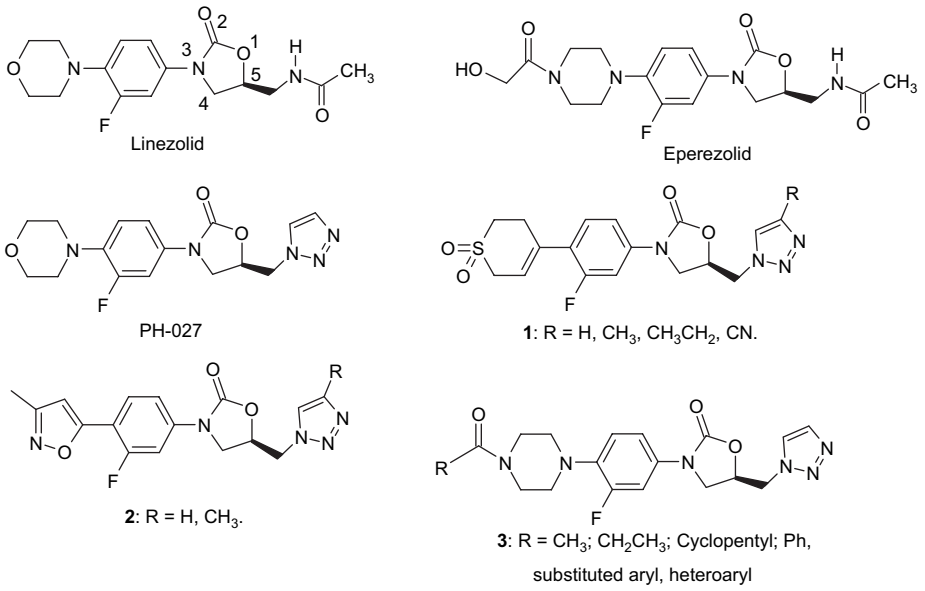

Fig. 1. Structures of antibacterial oxazolidinones.

elaborated on the structure–activity relationships of the piperazine derivatives similar to eperezolid, namely, the novel alkyl-(C_{1-5}) and 4-(phenylcarbonyl)piperazinyl 5-triazolylmethyl oxazolidinones **3** (Fig. 1), with improved antibacterial activity compared to the morpholine derivative PH-027 [16,17]. In addition, we have shown that substitution of the tolylsufonyl groups at the distal piperazine N-4-position resulted in diminished antibacterial activity [17]. In the present communication we investigated the effect of the alkyl group chain length at the distal piperazine N-4-position on the antibacterial activity. The structural variations were selected in order to investigate optimal structure–activity requirements for this novel class of 5-triazolylmethyl oxazolidinone derivatives **8a–o** and potential correlations between selected 3D molecular descriptors with the antibacterial activity. The molecular descriptors used, included lipophilicity reported as calculated log of partition coefficient (Clog *P* values), surface area (SA), molecular volume (MV), ovality, heat of formation (HOF), energies of the lowest unoccupied (E_{LUMO}) and the highest occupied (E_{HOMO}) molecular orbitals, dipole, and net charge on the nitrogen of the amide ($I_{NC=O}$), carbonyl carbon ($I_{NC=O}$), and oxygen atom ($I_{NC=O}$) at the distal piperazine N-4-position. We now report on the synthesis and structure–antibacterial activity of hitherto unreported long chain ($C_{n=5-18}$) alkylcarbonyl-oxazolidinones **8f–o**.

2. Chemistry

Compounds **8a–e** were previously reported [16], while the other derivatives **8f–o** were prepared as follows. The synthesis of the target compounds **8f–o** was carried out as outlined (Scheme 1) from the chiral alcohol derivative **6**, which was obtained in multi-step reactions in good yield according to published procedures [16,18]. Further chemical transformation of **6** to **7** involved the versatile Huisgen's 1,3 dipolar cycloaddition reaction [19] with acetylene in dimethoxyethane (DME) at 90 °C in excellent yield [16]. This was followed by the deprotection of the *tert*-butoxycarbonyl protecting group at the piperazine N-4-position with trifluoroacetic acid in CH_2Cl_2 at 0 °C to room temperature to give the key-intermediate triazole **7a** as a trifluoroacetic acid salt (quantitative). The intermediate triazole **7a** was subsequently reacted with appropriate long chain alkyl chlorides in MeCN, using triethylamine as base to give the respective target compounds **8f–n** in moderate to good yields. The bicyclo[2.2.1]heptan-2-yl acetyl derivative was prepared by reaction of the intermediate triazole **7b** with the activated bicyclo[2.2.1]heptan-2-yl acetic acid, which was obtained by the reaction with 1-hydroxybenzotriazole and dicyclohexylcarbodiimide in a mixture of CH_2Cl_2 and CH_3CN. All the compounds were characterized by their physical, analytical and spectroscopic data (^{1}H NMR, ^{13}C NMR, MS and IR) and melting points and were microanalyzed satisfactorily for C, H and N. Thorough structural verification of a representative compound **8f** was further performed by ^{13}C NMR decoupled, ^{13}C DEPT-135 (Distortionless enhancement by polarization transfer) and ^{13}C APT (Attached proton test) experiments.

3. Results and discussion

The C-5-triazolylmethyl oxazolidinones, exemplified by PH-027 are novel bioisoteres of the C-5-acetamidomethyl oxazolidinones, based on the similarities in the dipole moment and potential of the nitrogen atoms of the triazole and acetamide moieties to function as weak hydrogen bond acceptors [20]. Furthermore, the observed comparable or superior antibacterial activity [15,16] and reduced monoamine oxidase inhibitory activity [4,14,15] of the triazolyl derivatives **1** (Fig. 1) served as impetus for establishing the structure–antibacterial activity relationship of this class of compounds.

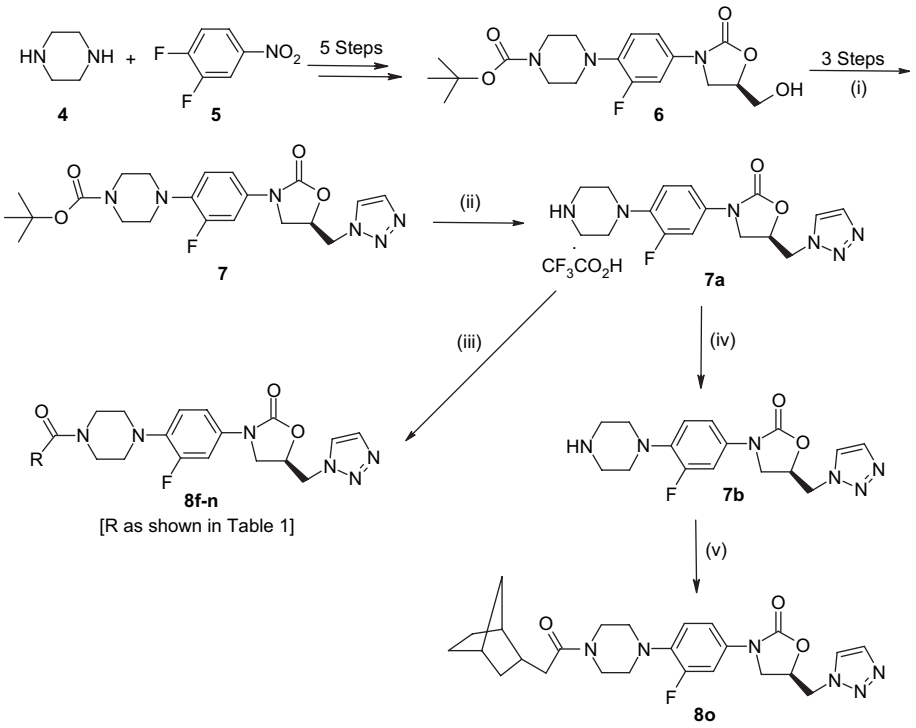

Scheme 1. Synthesis of acyl-piperazinyl oxazolidinone derivatives. (i) TEA, MsCl, CH_2Cl_2/DMF, NaN_3/acetylene, DME, 90 °C; (ii) TFA, 0 °C–rt, CH_2Cl_2; (iii) TEA, long chain alkylcarbonyl chlorides, 0 °C–rt, CH_3CN; (iv) $KHCO_3$ aq; (v) 2-Norbornaneacetic acid, DCC, 1-hydroxybenzotriazole, CH_2Cl_2–CH_3CN, rt.

The newly synthesized piperidinyl oxazolidinones (**8f–o**) having long acyl (C_{6-18}) groups appended to the nitrogen at the 4-position and the previously reported derivatives (**8a–e**) with shorter acyl groups were evaluated for antibacterial activity against a panel of standard and clinical isolates of Gram-positive and Gram-negative bacteria strains to investigate the effects of carbon chain length on antibacterial activity. Antibacterial activity was further evaluated against *S. aureus* ATCC 25923 standard strain in the presence and absence of 50% human plasma. The lipophilicity of the compounds is obtained as calculated log *P* (Clog *P*) [21], and the minimum inhibitory concentration (MIC, μg/ml) values and MIC distribution are presented in Tables 1 and 2, respectively.

Against all staphylococcal clinical isolates (MSSA, MRSA, MS-CNS, MR-CNS) the MIC values showed a consistent decrease in antibacterial activity as the number of carbon atoms in the alkyl chain length increases from compound **8a** ($R = CH_3$; Clog $P = -0.95$) to **8i** ($R = CH_3(CH_2)_7$; Clog $P = 2.50$) with MIC value ranges of 0.25–1 and 4 to >16 μg/ml (Table 1), respectively. Though increase in the antibacterial effects of a series of N-alkylated imidazole derivatives have been reported to correlate with increase in the number of carbon atoms in the alkyl chain up to nine carbons [22]. Moreover, other studies on a series of 1-alkyl-2-(4-pyridyl)pyridinium bromides have also demonstrated that compounds with alkyl chain length of between 11 and 16 carbon atoms are the most active [23]. Our data did not reveal similar findings in this class of oxazolidinone derivatives; rather a decrease in antibacterial activity was noticed with increase in carbon chain length, which somewhat correlated with increase in lipophilicity of the compounds.

Furthermore, compounds **8j–n** (Clog $P = 3.03–7.26$) with carbon atoms in the alkyl chain from nine and above showed higher MIC values (MIC > 16 μg/ml) against all standard and clinical strains tested, which is greater than the susceptibility break-point for linezolid (MIC ≤ 4 μg/ml) [24]. Similarly, all these long acyl derivatives showed cumulative 0% inhibition even at 16 μg/ml (Table 2) with the exception of compounds **8f** ($R = CH_3(CH_2)_4$; Clog $P = 0.91$), **8g** ($R = CH_3(CH_2)_5$; Clog $P = 1.44$), **8h** ($R = CH_3(CH_2)_6$; Clog $P = 1.97$) and the bicyclic derivative **8o** (R = bicyclo[2.2.1]heptan-2-yl)acetyl; Clog $P = 1.72$) that showed 100% cumulative inhibition of all staphylococcal strains tested at 4 and 8 μg/ml. In addition, compound **8o** (Clog $P = 1.72$), which contains an eight carbon atom relatively rigid bicyclic ring system showed improved antibacterial activity (MIC range 2–4 μg/ml) compared to derivative **8i** ($R = CH_3(CH_2)_7$; Clog $P = 2.50$) having similar number of carbon atoms, which was significantly less active (MIC range of 4 to >16 μg/ml) against all strains tested. This difference between the eight carbon atom derivatives **8i** and **8o**, could be due to the fact that the rigid bicyclo[2.2.1]heptane ring system in **8o** may favor formation of an active conformation, which is somewhat accessible to the active site, while the long acyl groups present in **8i** and other inactive derivatives **8j–n** facilitated adoption of bio-inactive conformations that may be inaccessible to the active site. Furthermore, the presence of the highly mobile long chain acyl groups could also introduce increased bulkiness at the terminal piperazinyl N-4-position with

Table 1
Comparative MIC (μg/ml) and Clog *P* values of acyl-piperazinyl oxazolidinones against Gram-positive standard strains and clinical isolates

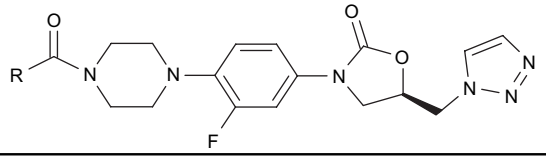

Compd	−R	Minimum inhibitory concentrations[a] (MICs, μg/ml) against									
		Clog *P*	*S. aureus*[b] w/o plasma[c]	*S. aureus*[b] + 50% plasma[c]	MSSA ($n=11$)	MRSA ($n=10$)	MS-CNS ($n=8$)	MR-CNS ($n=3$)	S. pn ($n=6$)	VSE ($n=7$)	VRE ($n=4$)
8a	CH_3[d]	−0.95	1	1	0.5−1	0.25−0.5	0.25−1	0.25−0.5	0.5−1	0.5−1	0.25
8b	CH_3CH_2[d]	−0.42	1	1	1	1	012−1	1	1	0.5−1	1
8c	$(CH_3)_2CH$−[d]	−0.11	2	2	1−2	1−2	1−2	1−2	0.5−1	1−2	1−2
8d	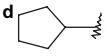	0.52	2	4	1−2	1−2	1−2	1−2	1−2	1−2	1−2
8e	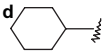	1.08	4	4	1−4	1−4	1−4	1−4	0.5−1	1−2	1−2
8f	$CH_3(CH_2)_4$	0.91	4	16	4	2−4	1−4	1−4	2−4	4	4
8g	$CH_3(CH_2)_5$	1.44	4	>16	2−4	2−8	1−4	2−4	4−8	4	4
8h	$CH_3(CH_2)_6$	1.97	8	>16	4−8	2−8	2−8	2−8	>16	4	4
8i	$CH_3(CH_2)_7$	2.50	>16	>16	8 to >16	4−16	4 to >16	4−8	>16	8	8
8j	$CH_3(CH_2)_8$	3.03	>16	>16	>16	>16	>16	>16	>16	>16	>16
8k	$CH_3(CH_2)_9$	3.56	>16	>16	>16	>16	>16	>16	>16	>16	>16
8l	$CH_3(CH_2)_{12}$	5.14	>16	>16	>16	>16	>16	>16	>16	>16	>16
8m	$CH_3(CH_2)_{14}$	6.20	>16	>16	>16	>16	>16	>16	>16	>16	>16
8n	$CH_3(CH_2)_{16}$	7.26	>16	>16	>16	>16	>16	>16	>16	>16	>16
8o	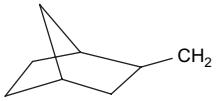	1.72	4	16	2−4	2−4	2−4	2−4	4	2−4	4
PH-027	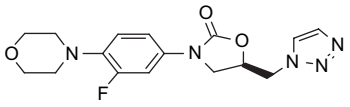	0.63	1	1	0.5−1	0.5−1	0.5−1	0.5−1	0.5−1	0.5−1	1
Lzd	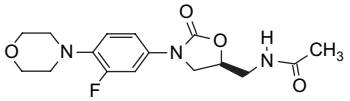	0.53 (0.55)[e]	2	2	1−2	0.5−2	0.25−2	1−2	0.5	0.5−2	2
Van		n/d	2	2	1−2	0.5−1	1−2	1	0.5	0.25−2	>64

[a] All compounds showed moderate to lack of activity against *H. influenzae*, *M. catarrhalis* and *E. coli*. (MIC = ≥8 μg/ml).
[b] ATCC 25923 strain.
[c] Human plasma (w/o: without plasma).
[d] Ref. [16].
[e] Pharmacia UpJohn, Material Safety Data Sheet for Linezolid (2000).

concomitant increase in lipophilicity of the molecules, which may possibly account for the diminished antibacterial potency. This could be consistent with established oxazolidinone SAR, which showed that excessive steric bulk on the aromatic ring at the phenyl C-3 and/or C-5 positions could be injurious to antibacterial activity [25]. From our data it was not possible to clearly conclude whether the diminished antibacterial activity was a result of increased lipophilicity or steric bulk. However, both factors may play significant roles. Moreover, it is evident that lipophilicity might be responsible for lack of antibacterial activity in presence of plasma, which could be due to plasma protein binding as Clog *P* values increase from **8f** (0.91) to **8n** (7.26) including compound **8o**. In all the long chain containing derivatives, a four fold increase or greater MIC values was observed in the presence of 50% plasma indicating plasma binding potentials.

Generally, a similar moderate to lack of antibacterial activity was observed for compounds **8f−o** against other Gram-positive clinical isolates including *S. pneumoniae*, VSE and VRE with MIC range of 2 to >16 μg/ml, compared with PH-027 (0.5−1 μg/ml), linezolid (0.5−2 μg/ml) and vancomycin (0.25−2; and >64 μg/ml for VRE). In addition, all the compounds were inactive against Gram-negative organisms evaluated in this study, which included *Haemophilus influenzae* and *Moraxella catarrhalis* clinical isolates and *Escherichia coli* ATCC 25922 (data not shown).

In order to gain insight into the structural requirements for antibacterial activity of these long chain acyl derivatives, we

Table 2
MIC (μg/ml) distribution of acyl-piperazinyl oxazolidinones against clinical isolates of staphylococci ($n = 32$)

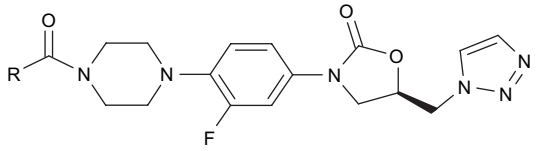

Compd	−R	Cumulative percent of isolates with specific MIC (μg/ml)						
		0.12	0.25	0.5	1	2	4	8
8a	CH_3-	0	45	83	100	100	100	100
8b	CH_3CH_2-	5	10	17	100	100	100	100
8c	$(CH_3)_2CH-$	0	0	0	36	100	100	100
8d		0	0	0	19	100	100	100
8e		0	0	0	33	55	100	100
8f	$CH_3(CH_2)_4$	0	0	0	6	13	100	100
8g	$CH_3(CH_2)_5$	0	0	0	6	28	100	100
8h	$CH_3(CH_2)_6$	0	0	0	0	16	79	100
8i	$CH_3(CH_2)_7$	0	0	0	0	0	16	72[a]
8j	$CH_3(CH_2)_8$	0	0	0	0	0	0	0[b]
8k	$CH_3(CH_2)_9$	0	0	0	0	0	0	0[b]
8l	$CH_3(CH_2)_{12}$	0	0	0	0	0	0	0[b]
8m	$CH_3(CH_2)_{14}$	0	0	0	0	0	0	0[b]
8n	$CH_3(CH_2)_{16}$	0	0	0	0	0	0	0[b]
8o	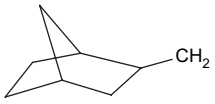	0	0	0	0	47	100	100
PH-027	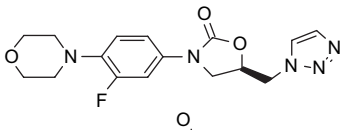	0	0	45	100	100	100	100
Lzd	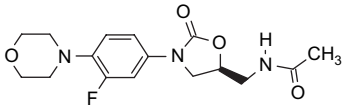	0	5	14	86	100	100	100
Van		0	0	24	93	100	100	100

[a] Showed MIC values of 16 and >16 μg/ml against 16% and 12% of the strains, respectively.
[b] Showed MIC values of >16 μg/ml against all strains tested.

decided to investigate potential correlations between antibacterial activity and selected molecular descriptors, the outcome of which may be helpful in predicting compounds that may assume potential bioactive conformation and binding orientations that may result in desirable activity. Prediction of bioactive conformations and binding orientations of ligands is not an easy task, since bioactive conformations may differ significantly from the unbound conformation [26]. We reasoned that any observable correlations might shed some light on SAR, which might be helpful in designing further structural modifications in this class of compounds, as suggested by other studies [27–29]. Therefore, we performed linear regression analyses for the Clog *P* [21], steric and selected molecular descriptors [30] with antibacterial activity. The antibacterial activity reported as MIC values (μg/ml, Tables 1 and 2), were transformed to pMIC (−log MIC) on a molar basis and used as dependent variables in correlation with molecular descriptors such as Clog *P*, surface area (SA), molecular volume (MV), ovality, heat of formation (HOF), energies of the lowest unoccupied (E_{LUMO}) and the highest occupied (E_{HOMO}) molecular orbitals, dipole, and net charge on the nitrogen of the amide ($I_{NC=O}$), carbonyl carbon ($I_{NC=O}$), and oxygen atom ($I_{NC=O}$) at the distal piperazine N-4-position (Table 3). These molecular descriptors were derived as described in the Section 4 of this manuscript.

The following conclusions could be deduced from the data: The activity of the compounds against the *S. aureus* and MRSA showed negative correlations ($r = -0.856$ and -0.836) to the Clog *P* values, since the activity decreased consistently with increase in Clog *P* values. Moreover, heat of formation correlated positively ($r = 0.846$, $p < 0.001$) with antibacterial activity. A similar correlation in a series of arylacryloylpiperazin-1-yl oxazolidinones has been reported [28], and affirmed that compounds with relatively high HOF (less −ve value) would show good activity. The heat of formation descriptor in QSAR model has been reported [28,29] to

Table 3
Molecular descriptors of acyl-piperazinyl oxazolidinones used in regression analyses

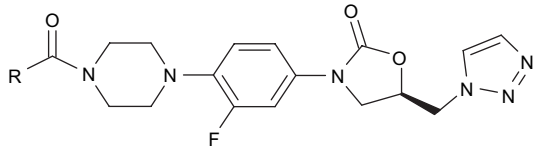

Compd	R	Clog *P*	log 1/MIC[a] (*S. aureus*[b])	log 1/MIC[a] (MRSA)	SA (A^2)	Ovality	MV (A^3)	E_{LUMO} (eV)	E_{HOMO} (eV)	Dipole MM3	HF	$I_{\underline{N}C=O}$ charge	$I_{N\underline{C}=O}$ charge	$I_{NC=\underline{O}}$ charge
8a	CH_3	−0.95	2.59	3.19	438.88	1.85	342.72	−10.51	−10.52	4.85	−19.98	−0.262	0.167	−0.421
8b	CH_3CH_2	−0.42	2.60	2.60	450.41	1.84	359.76	−10.51	−10.56	5.73	−28.89	−0.261	0.170	−0.420
8c	$(CH_3)_2CH-$	−0.11	2.32	2.62	465.41	1.86	370.76	−10.64	−10.80	4.95	−24.86	−0.262	0.173	−0.420
8d		0.52	2.34	2.65	504.99	1.92	400.08	−10.56	−10.65	5.50	−23.31	−0.261	0.173	−0.420
8e		1.08	2.06	2.66	525.76	1.95	416.09	−10.49	−10.49	3.16	−35.91	−0.261	0.173	−0.420
8f	$CH_3(CH_2)_4$	0.91	2.05	2.35	519.87	1.95	410.77	−10.37	−10.50	4.83	−45.43	−0.261	0.170	−0.420
8g	$CH_3(CH_2)_5$	1.44	2.06	2.36	532.85	1.96	421.27	−10.65	−10.85	5.19	−44.58	−0.016	0.231	−0.391
8h	$CH_3(CH_2)_6$	1.97	2.07	2.37	551.91	1.98	438.38	−10.62	−10.80	4.70	−44.95	−0.015	0.232	−0.391
8i	$CH_3(CH_2)_7$	2.50	1.78	2.09	596.59	2.06	462.70	−10.48	−10.50	4.06	−39.79	−0.261	0.170	−0.420
8j	$CH_3(CH_2)_8$	3.03	1.50	1.50	621.09	2.10	479.55	−10.52	−10.53	0.43	−68.23	−0.261	0.170	−0.420
8k	$CH_3(CH_2)_9$	3.56	1.51	1.51	638.55	2.11	496.34	−10.51	−10.55	0.89	−75.24	−0.261	0.170	−0.420
8l	$CH_3(CH_2)_{12}$	5.14	1.54	1.54	682.33	2.13	539.27	−10.63	−10.80	5.67	−84.57	−0.263	0.170	−0.420
8m	$CH_3(CH_2)_{14}$	6.20	1.56	1.56	747.59	2.22	580.72	−10.51	−10.52	3.81	−84.96	−0.261	0.078	−0.420
8n	$CH_3(CH_2)_{16}$	7.26	1.58	1.58	781.76	2.25	609.47	−10.65	−10.82	5.36	−102.43	−0.007	0.078	−0.396
8o	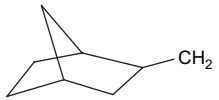	1.72	2.08	2.38	533.40	1.93	433.63	−10.64	−10.76	5.56	−22.87	−0.261	0.078	−0.420
Epzd	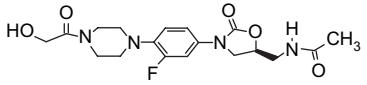	−1.09	n/d	n/d	431.72	1.82	343.79	−10.98	−11.46	3.74	−108.05	−0.015	0.214	−0.358
PH-027	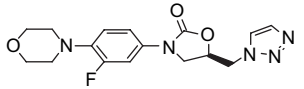	0.63	n/d	n/d	392.87	1.80	302.04	−10.46	−10.50	4.47	1979.78	n/a	n/a	n/a
Lzd	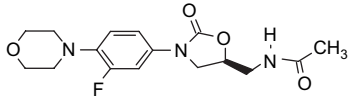	0.53	n/d	n/d	372.03	1.73	295.28	−10.95	−11.47	1.11	1864.19	n/a	n/a	n/a

SA: surface area; MV: molecular volume; HF: heat of formation (kcal/mol); n/d: not determined; n/a: not applicable.
[a] Lower MIC values.
[b] ATCC 25923 strain.

indicate conformational stability, which may favor better binding and improved activity at the molecular level. In our study, no correlation could be established with E_{LUMO}, an electronic parameter that measures electrophilicity of the molecule. This finding is contrary to a previous report on the arylacryloylpiperazin-1-yl oxazolidinones series, which indicated that compounds with high heats of formation and low E_{LUMO} (highly −ve value) would show good antibacterial activity [28]. Similarly no correlation with antibacterial activity was observed for E_{HOMO}, dipole and net charge on the nitrogen of the amide ($I_{NC=O}$), carbonyl carbon ($I_{NC=O}$), and oxygen atom ($I_{NC=O}$) at the distal piperazine N-4-position. This is in agreement with findings from previous studies [28,29].

In conclusion, a series of piperazinyl oxazolidinones having long chain acyl groups at the distal piperazinyl N-4-position were synthesized and evaluated for antibacterial activity. Attempts were made to correlate antibacterial activity with selected molecular descriptors. Activity was observed to decrease with increase in carbon chain length with significant decrease in antibacterial activity with compounds having nine carbon atoms or more. In general, antibacterial activity correlated positively to the heat of formation of the compounds, which has been suggested to indicate favorable conformational stability and better binding and activity at the receptor site. On the other hand, the activity of the compounds correlated negatively with Clog *P* values, surface area, ovality and molecular volume, suggesting consistent decrease in activity with increase in the size of the acyl chain. However, no significant correlation was observed between activity and E_{LUMO}, E_{HOMO} and dipole, respectively. This study contributes to the understanding of the structure–antibacterial activity requirements for this novel class of compounds, and highlights vital molecular descriptors that could be used in designing novel and more active derivatives.

4. Experimental

All common reagents and solvents were obtained from commercial sources and used without further purification. Extracted solvents were dried over anhydrous Na_2SO_4, followed by evaporation *in vacuo*, and column chromatography was carried out with silica gel (Kieselgel 60, 70–230 mesh; Aldrich). TLC was conducted on 0.25 mm pre-coated silica gel plates ($60F_{254}$, Merck). Melting points were determined on a Stuart Scientific SMP1 melting point apparatus and are uncorrected. The Science Analytical Facilities (SAF), Faculty of Science, Kuwait University, performed all the instrumental analyses. ^{1}H NMR spectra for all compounds were recorded on Bruker DPX 400 NMR spectrometer using DMSO-d_6 as solvent and tetramethylsilane (TMS) as an internal reference, and chemical shifts were reported in ppm. ^{13}C NMR spectrum of representative compound **8f** was recorded on Bruker Avance II 600 NMR spectrometer using DMSO-d_6 as solvent and tetramethylsilane (TMS) as an internal reference, and chemical shifts were reported in ppm. The mass spectrometry measurements were performed on a Finnigan MAT INCOS XL mass spectrometer. Infrared (IR) spectra were recorded on Perkin Elmer System 2000 FT-IR spectrometer. Elemental analyses were performed on a LECO elemental analyzer CHNS 932 apparatus, and analyses indicated by the symbols of the elements were within ±0.4% of the theoretical values.

The structures of the synthesized oxazolidinone derivatives **8a–o** were sketched using ChemDraw Ultra 8.0 [21] and were exported to Alchemy 2000 (Alchemy32) 2.05 [30]. Three dimensional (3D) structures of the molecules were generated and saved for database processing using geometry optimization method. The following molecular descriptors were obtained for the entire molecule: surface area (SA), molecular volume (MV), ovality, heat of formation (HOF), energy of the lowest unoccupied (E_{LUMO}) and the highest occupied (E_{HOMO}) molecular orbitals, dipole, and net charge on the nitrogen of the amide ($I_{NC=O}$), carbonyl carbon ($I_{NC=O}$), and carbon oxygen atom ($I_{NC=O}$) at the distal piperazine N-4-position. The Clog *P* values were calculated using ChemDraw Ultra 8.0. Nonparametric Spearman's correlation coefficient was performed using SPSS v13.0 at $p < 0.001$.

5. Syntheses

5.1. General procedure for the long chain alkylcarbonyl-oxazolidinones *8f–n*

A solution of the 5-((1*H*-1,2,3-triazol-1-yl)methyl)-3-(3-fluoro-4-(piperazinium-1-yl) phenyl)oxazolidin-2-one trifluoroacetic acid salt **7a** (1.00 g, 2.17 mmol) in acetonitrile (10 ml) cooled to 0 °C was treated with triethylamine (1 ml) and an appropriate long chain alkylcarbonyl chloride (3.26 mmol) and stirred to room temp overnight. Dichloromethane (20 ml) was added to the reaction mixture and the solution was washed with water (3 × 10 ml). The organic layer was washed with brine, dried (anhydrous Na_2SO_4), filtered and concentrated to give a solid, which was triturated with ether to give a solid. The crude solid was recrystallized in appropriate solvent systems to give the pure products.

5.1.1. (R)-5-((1H-1,2,3-Triazol-1-yl)methyl)-3-(3-fluoro-4-(4-hexanoylpiperazin-1-yl) phenyl)oxazolidin-2-one *8f*

Prepared according to the general procedure. Recrystallization from MeCN afforded a crystalline solid (381 mg, 39%, yield), mp 194–195 °C. ^{1}H NMR (DMSO-d_6): δ 8.17 (s, 1H, triazole H), 7.77 (s, 1H, triazole H), 7.42 (dd, 1H, $J = 2.3$ Hz, 14.7 Hz, phenyl H), 7.13 (dd, 1H, $J = 2.1$ Hz, 9.0 Hz, phenyl H), 7.06 (t, 1H, $J = 9.0$ Hz, phenyl H), 5.09–5.14 (m, 1H, CH_2CHCH_2–N–N=N), 4.83 (d, 2H, $J = 5.0$ Hz, CH_2CHCH_2–N–N=N), 4.20 (t, 1H, $J = 9.2$ Hz, $CHHCHCH_2$–N–N=N), 3.86 (dd, 1H, $J = 5.7$ Hz, 9.2 Hz, $CHHCHCH_2$–N–N=N), 3.59 (s, 4H, piperazine H), 2.90–2.96 (m, 4H, piperazine H), 2.33 (t, 2H, $J = 7.5$ Hz, $CH_3CH_2CH_2CH_2CH_2CO$), 1.47–1.54 (m, 2H, $CH_3CH_2CH_2CH_2CH_2CO$), 1.27–1.29 (m, 4H, $CH_3CH_2CH_2CH_2CH_2CO$), 0.87 (t, 3H, $J = 6.7$ Hz, $CH_3CH_2CH_2CH_2CH_2CO$). ^{13}C NMR (600 MHz, DMSO-d_6): δ 13.86, 21.93, 24.46, 30.98, 32.14, 40.93, 44.96, 47.06, 50.28, 50.73, 51.68, 70.75, 106.63, 106.80, 114.23, 114.24, 119.70, 119.73, 125.83, 133.23,

153.72, 170.65. IR (KBr pellet, cm^{-1}): ν 2958, 2920, 2855, 1749, 1623, 1518, 1438, 1417, 1325, 1224, 1111, 1036. *m/z* 444.6 (M^+). Anal CHNS: calc C 59.44, H 6.58, N 18.91, found: C 59.25, H 5.90, N 18.62.

5.1.2. (R)-5-((1H-1,2,3-Triazol-1-yl)methyl)-3-(3-fluoro-4-(4-heptanoylpiperazin-1-yl) phenyl)oxazolidin-2-one **8g**

Prepared according to the general procedure. Recrystallization from MeCN afforded a crystalline solid (559 mg, 56%, yield), mp 175–177 °C. ^1H NMR (DMSO-d_6): δ 8.17 (s, 1H), 7.77 (s, 1H), 7.42 (dd, 1H, $J = 2.3$ Hz, 14.7 Hz), 7.13 (dd, 1H, $J = 2.0$ Hz, 9.0 Hz), 7.06 (t, 1H, $J = 9.0$ Hz), 5.10–5.16 (m, 1H), 4.83 (d, 2H, $J = 5.0$ Hz), 4.20 (t, 1H, $J = 9.2$ Hz), 3.86: (dd, 1H, $J = 5.7$ Hz, 9.2 Hz), 3.59 (s, 4H), 2.93 (m, 4H), 2.33 (t, 2H, $J = 7.5$ Hz), 1.47–1.52 (m, 2H), 1.27–1.31 (m, 4H), 0.87 (t, 3H, $J = 6.7$ Hz). IR (KBr pellet, cm^{-1}): ν 2856, 2926, 1746, 1628, 1518, 1463, 1436, 1417, 1327, 1225, 1195, 1113, 1099, 1040. *m/z* 458.4 (M^+). Anal CHNS: calc C 60.25, H 6.81, N 18.33, found C 60.08, H 6.36, N 18.51.

5.1.3. (R)-5-((1H-1,2,3-Triazol-1-yl)methyl)-3-(3-fluoro-4-(4-octanoylpiperazin-1-yl) phenyl)oxazolidin-2-one **8h**

Prepared according to the general procedure. Recrystallization from MeCN afforded a crystalline solid (567 mg, 55%, yield), mp 150–152 °C. ^1H NMR (DMSO-d_6): δ 8.17 (s, 1H), 7.77 (s, 1H), 7.42 (dd, 1H, $J = 2.3$ Hz), 7.13 (dd, 1H, $J = 2.1$ Hz, 9.0 Hz), 7.06 (t, 1H, $J = 9.0$ Hz), 5.11–5.14 (m, 1H), 4.83 (d, 2H, $J = 5.0$ Hz), 4.21 (t, 1H, $J = 9.2$ Hz), 3.86 (dd, 1H, $J = 5.7$ Hz, 9.2 Hz), 3.59 (s, 4H), 2.90–2.95 (m, 4H), 2.33 (t, 2H, $J = 7.5$ Hz), 1.49–1.52 (m, 2H), 1.28 (m, 8H), 0.87 (t, 3H, $J = 6.7$ Hz). IR (KBr pellet, cm^{-1}): ν 2922, 2853, 1740, 1636, 1523, 1443, 1418, 1327, 1283, 1163, 1026. *m/z* 472.4 (M^+). Anal CHNS: calc C 60.99, H 7.04, N 17.79, found C 60.79, H 6.57, N 17.93.

5.1.4. (R)-5-((1H-1,2,3-Triazol-1-yl)methyl)-3-(3-fluoro-4-(4-nonanoylpiperazin-1-yl) phenyl)oxazolidin-2-one **8i**

Prepared according to the general procedure. Recrystallization from MeCN afforded a crystalline solid (340 mg, 32%, yield), mp 133–135 °C. ^1H NMR (DMSO-d_6): δ 8.17 (s, 1H), 7.77 (s, 1H), 7.42 (dd, 1H, $J = 2.3$ Hz, 14.7 Hz), 7.13 (dd, 1H, $J = 2.0$ Hz, 9.0 Hz), 7.06 (t, 1H, $J = 9.0$ Hz), 5.11–5.14 (m, 1H), 4.83 (d, 2H, $J = 5.0$ Hz), 4.21 (t, 1H, $J = 9.0$ Hz), 3.86 (dd, 1H, $J = 5.7$ Hz, 9.2 Hz), 3.59 (s, 4H), 2.90–2.95 (m, 4H), 2.33 (t, 2H, $J = 7.5$ Hz), 1.49–1.52 (m, 2H), 1.28 (m, 10H), 0.86 (t, 3H, $J = 6.6$ Hz). IR (KBr pellet, cm^{-1}): ν 2927, 2853, 1740, 1638, 1523, 1443, 1418, 1328, 1220, 1032. *m/z* 486.1 (M^+). Anal CHNS: calc C 61.71, H 7.25, N 17.27, found C 61.59, H 7.22, N 17.30.

5.1.5. (R)-5-((1H-1,2,3-Triazol-1-yl)methyl)-3-(4-(4-decanoylpiperazin-1-yl)-3-fluoro phenyl)oxazolidin-2-one **8j**

Prepared according to the general procedure. Recrystallization from MeCN afforded a crystalline solid (490 mg, 45%, yield), mp 138–140 °C. ^1H NMR (DMSO-d_6): δ 8.17 (s,1H), 7.77 (s,1H), 7.42 (dd,1H, $J = 2.2$ Hz, 14.7 Hz), 7.13 (dd, 1H, $J = 2$ Hz, 9.0 Hz), 7.06 (t, 1H, $J = 9.0$ Hz), 5.11–5.14 (m, 1H), 4.83 (d, 2H, $J = 5.0$ Hz), 4.21 (t, 1H, $J = 9.2$ Hz), 3.86 (dd, 1H, $J = 5.7$ Hz, 9.2 Hz), 3.59 (s, 4H), 2.90–2.95 (m, 4H), 2.33 (t, 2H, $J = 7.4$ Hz), 1.50 (m, 2H), 1.26 (br s, 12H), 0.86 (t, 3H, $J = 6.7$ Hz). IR (KBr pellet, cm^{-1}): ν 2922, 2851, 1739, 1637, 1523, 1419, 1384, 1223, 1138, 1036. *m/z* 500.2 (M^+). Anal CHNS: calc C 62.38, H 7.45, N 16.79, found C 62.07, H 7.39, N 16.83.

5.1.6. (R)-5-((1H-1,2,3-Triazol-1-yl)methyl)-3-(3-fluoro-4-(4-undecanoylpiperazin-1-yl)phenyl)oxazolidin-2-one **8k**

Prepared according to the general procedure. Recrystallization from MeCN and EtOAc afforded a crystalline solid (280 mg, 50%, yield), mp 149–151 °C. ^1H NMR (DMSO-d_6): δ 8.18 (s, 1H), 7.77 (s, 1H), 7.42 (dd, 1H, $J = 2.3$ Hz, 14.7 Hz), 7.13 (dd, 1H, $J = 2.2$ Hz, 9.0 Hz), 7.06 (t, 1H, $J = 9.0$ Hz), 5.11–5.14 (m, 1H), 4.83 (d, 2H, $J = 5.0$ Hz), 4.21 (t, 1H, $J = 9.2$ Hz), 3.86 (dd, 1H, $J = 5.7$ Hz, 9.2 Hz), 3.59 (s, 4H), 2.90–2.95 (m, 4H), 2.33 (t, 2H, $J = 7.5$ Hz), 1.50 (m, 2H), 1.25 (br. s, 14H), 0.86 (t, 3H, $J = 6.6$ Hz). IR (KBr pellet, cm^{-1}): ν 2922, 2851, 1738, 1636, 1522, 1418, 1223, 1190, 1163, 1038. *m/z* 514.2 (M^+). Anal CHNS: calc C 63.01, H 7.64, N 16.33, found C 62.92, H 7.61, N 16.16.

5.1.7. (R)-5-((1H-1,2,3-Triazol-1-yl)methyl)-3-(3-fluoro-4-(4-tetradecanoylpiperazin-1-yl)phenyl)oxazolidin-2-one **8l**

Prepared according to the general procedure. Recrystallization from MeCN afforded a crystalline solid (392 mg, 65%, yield), mp 157–159 °C. ^1H NMR (DMSO-d_6): δ 8.18 (s, 1H), 7.77 (s, 1H), 7.42 (dd, 1H, $J = 2.3$ Hz, 14.7 Hz), 7.13 (dd, 1H, $J = 2.2$ Hz, 9.0 Hz), 7.05 (t, 1H, $J = 9.0$ Hz), 5.11–5.14 (m, 1H), 4.83 (d, 2H, $J = 5.0$ Hz), 4.20 (t, 1H, $J = 9.0$ Hz), 3.86 (dd, 1H, $J = 5.7$ Hz, 9.2 Hz), 3.59 (s, 4H), 2.90–2.95 (m, 4H), 2.33 (t, 2H, $J = 7.5$ Hz), 1.49 (m, 2H), 1.24 (br. s, 20H), 0.86 (t, 3H, $J = 6.7$ Hz). IR (KBr pellet, cm^{-1}): ν 2920, 2851, 1738, 1637, 1524, 1420, 1221, 1163, 1028. *m/z* 556.4 (M^+). Anal CHNS: calc C 64.72, H 8.15, N 15.10, found C 64.52, H 8.02, N 15.10.

5.1.8. (R)-5-((1H-1,2,3-Triazol-1-yl)methyl)-3-(3-fluoro-4-(4-palmitoylpiperazin-1-yl) phenyl)oxazolidin-2-one **8m**

Prepared according to the general procedure. Recrystallization from MeCN afforded a crystalline solid (290 mg, 23%, yield), mp 155–156 °C. ^1H NMR (DMSO-d_6): δ 8.18 (s, 1H), 7.77 (s, 1H), 7.42 (dd, 1H, $J = 2.3$ Hz, 14.7 Hz), 7.13 (dd, 1H, $J = 2.2$ Hz, 9.0 Hz), 7.06 (t, 1H, $J = 9.0$ Hz), 5.11–5.14 (m, 1H), 4.83 (d, 2H, $J = 5.0$ Hz), 4.21 (t, 1H, $J = 9.2$ Hz), 3.86 (dd, 1H, $J = 5.7$ Hz, 9.2 Hz), 3.59 (s, 4H), 2.90–2.95 (m, 4H), 2.33 (t, 2H, $J = 7.5$ Hz), 1.49 (br. s, 2H), 1.24 (br. s, 22H), 0.86 (t, 3H, $J = 6.6$ Hz). IR (KBr pellet, cm^{-1}): ν 2920, 2851, 1738, 1637, 1524, 1420, 1225, 1165, 1035. *m/z* 584.5 (M^+). Anal CHNS: calc C 65.73, H 8.45, N 14.38, found C 65.63, H 8.37, N 14.47.

5.1.9. (R)-5-((1H-1,2,3-Triazol-1-yl)methyl)-3-(3-fluoro-4-(4-stearoylpiperazin-1-yl)phenyl)oxazolidin-2-one ***8n***

Prepared according to the general procedure. Recrystallization from MeCN afforded a crystalline solid (398 mg, 60%, yield), mp 148–149 °C. ^{1}H NMR (DMSO-d_6): δ 8.18 (s, 1H), 7.77 (s, 1H), 7.42 (dd, 1H, $J = 2.3$ Hz, 14.7 Hz), 7.13 (dd, 1H, $J = 2.2$ Hz, 9.0 Hz), 7.06 (t, 1H, $J = 9.0$ Hz), 5.11–5.14 (m, 1H), 4.83 (d, 2H, $J = 5.0$ Hz), 4.21 (t, 1H, $J = 9.2$ Hz), 3.86 (dd, 1H, $J = 5.7$ Hz, 9.2 Hz), 3.59 (s, 4H), 2.90–2.95 (m, 4H), 2.33 (t, 2H, $J = 7.5$ Hz), 1.50 (m, 2H), 1.24 (br. s, 28H), 0.86 (t, 3H, $J = 6.6$ Hz). IR (KBr pellet, cm^{-1}): ν 2918, 2851, 1738, 1639, 1524, 1421, 1225, 1161, 1026. *m/z* 612.6 (M^+). Anal CHNS: calc C 66.63, H 8.72, N 13.72, found C 66.62, H 8.75, N 13.20.

5.1.10. (R)-5-((1H-1,2,3-Triazol-1-yl)methyl)-3-(4-(4-(2-(bicyclo[2.2.1]heptan-2-yl)acetyl) piperazin-1-yl)-3-fluorophenyl) oxazolidin-2-one ***8o***

The trifluoroacetic acid salt **7a** (1.50 g, 6.52 mmol) was triturated with a saturated potassium carbonate solution (10 ml), and the precipitate was collected and dried to give the free base **7b** (0.930 g). In a separate flask, a solution of 2-norbornaneacetic acid (1.00 g, 0.939 ml, 6.49 mmol) in DCM (20 ml) was treated with dicyclohexyl carbodimide (1.61 g, 7.78 mmol) and 1-hydroxybenzotriazole (1.05 g, 7.78 mmol). The reaction mixture was stirred at room temperature for 2 h and was filtered directly into a flask containing a solution of the free base **7b** in MeCN. The reaction mixture was stirred at room temperature overnight. The mixture was concentrated, redissolved in ethyl acetate and washed with water, brine, and the organic layer was dried (Na_2SO_4). Recrystallization from MeCN–EtOAc afforded a crystalline solid (448 mg, 35%, yield), mp 177–179 °C. ^{1}H NMR (DMSO-d_6, 400 MHz): δ 8.18 (s, 1H), 7.77 (s, 1H), 7.42 (dd, 1H, $J = 2.0$ Hz, 15.0 Hz), 7.13 (dd, 1H, $J = 2.0$ Hz, 9.0 Hz), 7.06 (t, 1H, $J = 9.0$ Hz), 5.11–5.14 (m, 1H), 4.83 (d, 2H, $J = 5.0$ Hz), 4.21 (t, 1H, $J = 9.0$ Hz), 3.86 (dd, 1H, $J = 6.0$ Hz, 9.0 Hz), 3.59 (br. s, 4H), 2.90–2.95 (m, 4H), 2.33 (dd, 1H, $J = 8.0$ Hz, 15.0 Hz), 2.18 (dd, 1H, $J = 8.0$ Hz, 15.0 Hz, overlaps partly with br. s, at 2.17), 2.17 (br. s, 1H), 1.95 (br. s 1H), 1.83–1.80 (m, 1H), 1.46–1.34 (m, 4H), 1.17–1.03 (m, 4H). IR (KBr pellet, cm^{-1}): ν 2948, 2853, 1742, 1630, 1521, 1441, 1420, 1325, 1224, 1035. *m/z* 482 (M^+). Anal calc for $C_{25}H_{31}FN_6O_3$: C 62.22, H 6.48, N 17.42, found C 62.60, H 6.96, N 17.11.

6. Microbiology

6.1. Antibacterial susceptibility testing

The clinical isolates used in the study were obtained from culture collection maintained at the MRSA Reference Laboratory, Faculty of Medicine, Kuwait University. Antibacterial susceptibility testing was performed by the agar dilution method according to the Clinical and Laboratory Standard Institute (CSLI) (formerly National Committee for Clinical Laboratory Standards) [31]. Minimum inhibitory concentrations (MICs, μg/ml) were determined on Mueller–Hinton (MH) agar with medium containing dilutions of antibacterial agents ranging from 0.12 to 16 μg/ml, and up to 64 μg/ml for vancomycin against enterococci. The test compounds were dissolved in 20% water in DMSO, while linezolid and vancomycin were dissolved in 40% water in ethanol and water, respectively. The tests were performed using MH agar plates for all staphylococci and enterococci, and on MH agar plates supplemented with 5% sheep blood to facilitate the growth of *S. pneumoniae*, *H. influenzae* and *M. catarrhalis*. The Gram-positive organisms utilized in this study consisted of methicillin-resistant *S. aureus* (MRSA, $n = 10$), methicillin-susceptible *S. aureus* (MSSA, $n = 11$), methicillin-resistant coagulase-negative staphylococci (MR-CNS, $n = 3$), methicillin-sensitive coagulase-negative staphylococci (MS-CNS, $n = 8$), *S. pneumoniae* ($n = 6$), vancomycin-sensitive (VSE, $n = 7$) and vancomycin-resistant (VRE, $n = 4$) enterococci. The Gram-negative organisms tested included *H. influenzae* ($n = 5$) and *M. catarrhalis* ($n = 3$) clinical isolates; and *E. coli* ATCC 25922. The reference strains, *S. aureus* ATCC 25923, *Staphylococcus epidermidis* ATCC 12228 and *Enterococcus faecalis* ATCC 29212, *E. coli* ATCC 25922 and *H. influenzae* ATCC 49247 were used as controls. The final bacterial concentration for inocula was 10^7 CFU/ml, and was incubated at 35 °C for 18 h. The test compounds were also evaluated against *S. aureus* ATTC 25923 in MH broth supplemented with 50% human plasma. The MIC was defined as the lowest drug concentration that completely inhibited growth of the bacteria. PH-027, prepared according to literature methods [13], and linezolid and vancomycin obtained from commercial sources were used as reference antibacterial agents.

Acknowledgment

This work was supported by the Research Administration, Kuwait University Research Grant PC01/02 (OAP), and Instrument Grants GS01/01, GS03/01 and GS01/03 awarded to the Science Analytical Facilities (SAF). Thanks to Dr. Prem Sharma, Health Sciences Computer Center, Kuwait University for performing the statistical analysis.

References

[1] F. Blasi, P. Braga, M. Cazzola, R. Cosentini, P. Tarsia, Expert Opin. Investig. Drugs 11 (4) (2002) 545–552.
[2] T.S. Lundstrom, J.D. Sobel, Infect. Dis. Clin. North Am. 18 (2004) 651–668.
[3] D.K. Hutchinson, Curr. Top. Med. Chem. 3 (2003) 1021–1042.
[4] M.B. Gravestock, Curr. Opin. Drug Discov. Devel. 8 (4) (2005) 469–477.
[5] D. Styers, D.J. Sheehan, P. Hogan, D.F. Sahn, Ann. Clin. Microbiol. Antimicrob. 5 (2006) 2 (Online journal published by Biomed Central).
[6] B. Bozdogan, P.C. Appelbaum, Int. J. Antimicrob. Agents 23 (2) (2004) 113–119.
[7] A. Sinclair, C. Arnold, N. Woodford, Antimicrob. Agents Chemother. 47 (11) (2003) 3620–3622.
[8] C.C. Zhou, S.M. Swaney, D.L. Shinabarger, B.J. Stockman, Antimicrob. Agents Chemother. 46 (2002) 625–629.
[9] S. Tsiodras, H.S. Gold, G. Sakoulas, G.M. Eliopoulos, C. Wennersten, L. Venkataraman, R.B. Moellering Jr., M.J. Ferraro, Lancet 358 (2001) 207–208.

[10] R.D. Gonzales, P.C. Schreckenberger, M.B. Graham, S. Kelkar, K. DenBesten, J.P. Quinn, Lancet 357 (9263) (2001) 1179.
[11] A.P. Johnson, L. Tysall, M.W. Stockdale, N. Woodford, M.E. Kaufmann, M. Warner, D.M. Livermore, F. Asboth, F.J. Allerberger, Eur. J. Clin. Microbiol. Infect. Dis. 21 (2001) 751–754.
[12] S. Rahim, K. Pillai, H.S. Gold, L. Venkataraman, K. Inglima, R.A. Press, Clin. Infect. Dis. 36 (2003) e146–e148.
[13] O.A. Phillips, E.E. Udo, A.A.M. Ali, N. Al-Hassawi, Bioorg. Med. Chem. 11 (2003) 35–41.
[14] F. Reck, F. Zhou, M. Girardot, G. Kern, C.J. Eyermann, N.J. Hales, R.R. Ramsay, M.B. Gravestock, J. Med. Chem. 48 (2005) 499–506.
[15] S.I. Hauck, C. Cederberg, A. Doucette, L. Grosser, N.J. Hales, G. Poon, M.B. Gravestock, Bioorg. Med. Chem. Lett. 17 (2007) 337–340.
[16] O.A. Phillips, E.E. Udo, A.A.M. Ali, S.M. Samuel, Bioorg. Med. Chem. 13 (2005) 4113–4123.
[17] O.A. Phillips, E.E. Udo, A.A.M. Ali, S.M. Samuel, Eur. J. Med. Chem. 42 (2007) 214–225.
[18] S.J. Brickner, D.K. Hutchinson, M.R. Barbachyn, P.R. Manninen, D.A. Ulanowicz, S.A. Garmon, K.C. Grega, S.K. Hendges, D.S. Toops, C.W. Ford, G.E. Zurenko, J. Med. Chem. 39 (1996) 673–679.
[19] R. Huisgen, in: A. Padwa (Ed.), 1,3 Dipolar Cycloaddition – Introduction, Survey, Mechanism, 1,3 Dipolar Cycloaddition Chemistry, vol. 1, Wiley, New York, 1984, pp. 1–176.
[20] H.C. Kolb, K.B. Sharpless, Drug Discov. Today 8 (4) (2003) 1128–1137.
[21] Calculated log *P* (Clog *P*) values were computed by using the CS ChemDraw Ultra ver. 8.0.3, September 24, 2003 by CambridgeSoft.Com, Cambridge, MA, USA.
[22] S. Khabnadideh, Z. Rezaei, A. Khalafinegad, R. Bahrinajafi, R. Mohamadi, A.A. Farrokhroz, Bioorg. Med. Chem. Lett. 13 (17) (2003) 2863–2865.
[23] B.J. Denny, L. Novotny, P.W.J. West, M. Blesova, J. Zamocka, Med. Princ. Pract. 14 (2005) 377–381.
[24] European Committee on Antimicrobial Susceptibility Testing (EUCAST) of the European Society of Clinical Microbiology and Infections Diseases (ESCMID), Linezolid breakpoints, Clin. Micobiol. Infect. 7 (5) (2001) 283–284.
[25] C.H. Park, D.R. Brittelli, C.L. Wang, F.D. Marsh, W.A. Gregory, M.A. Wuonola, R.J. McRipley, V.S. Eberly, A.M. Slee, M. Forbes, J. Med. Chem. 35 (6) (1992) 1156–1165.
[26] F. Leclerc, R. Cedergren, J. Med. Chem. 41 (2) (1998) 175–182.
[27] A.N. Pae, S.Y. Kim, H.Y. Kim, H.J. Joo, Y.S. Cho, K.I. Choi, J.H. Choi, H.Y. Koh, Bioorg. Med. Chem. Lett. 9 (1999) 2685–2690.
[28] B.B. Lohray, N. Gandhi, B.K. Srivastava, V.B. Lohray, Bioorg. Med. Chem. Lett. 16 (2006) 3817–3823.
[29] N. Zanatta, S.H. Alves, H.S. Coelho, D.M. Borchhardt, P. Machado, K.M. Flores, F.M. da Silva, T.B. Spader, J.M. Santurio, H.G. Bonacorso, M.A.P. Martins, Bioorg. Med. Chem. 15 (2007) 1947–1958.
[30] Structural descriptors were computed by using Alchemy 2000 (Alchemy32) ver. 2.0.5, Tripos, USA.
[31] National Committee for Clinical Laboratory Standards, Methods for Dilution Antimicrobial Susceptibility Tests for Bacteria that Grow Aerobically, Approved Standard. NCCLS Document M7–A4, fourth ed. National Committee for Clinical Laboratory Standards, Villanova, PA, 1997.